

Adsorption of 1-Octanethiol on the GaN(0001) Surface

V. M. Bermudez*

Naval Research Laboratory, 4555 Overlook Avenue SW, Washington, D.C. 20375-5347

Received January 27, 2003. In Final Form: April 30, 2003

The chemisorption of 1-octanethiol [CH₃(CH₂)₆CH₂SH] from the vapor phase on the GaN(0001)–(1 × 1) surface has been studied using X-ray photoemission, ultraviolet photoemission, and X-ray-excited Auger electron spectroscopies. Quantitative analysis of relative peak intensities indicates that the molecule adsorbs via the thiol group with a saturation coverage of ~0.28 monolayers and with the alkyl chain lying essentially parallel to the surface. Upon annealing, most of the alkyl C desorbs by ~350 °C, but most of the S remains. Little or no indication of X-ray-induced damage in the adsorbed thiol layer is seen during data collection.

Introduction

The adsorption of *n*-alkanethiols on metal and semiconductor substrates has been extensively studied^{1–4} in the context of well-ordered, self-assembled monolayers (SAMs) and as models for ordered organic surfaces. Here, we consider thiol adsorption on the relatively new, wide-band-gap semiconductor ($E_g = 3.4$ eV) GaN. In addition to the many well-known⁵ applications for such hybrid organic/semiconductor interfaces, there are further reasons for interest in this system.

First, the chemistry needed to “functionalize” (i.e., attach organic ligands to) the GaN(0001)–(1 × 1) surface is still being developed.⁶ On the basis of the high reactivity of H₂O with this surface,⁷ organic alcohols are expected to chemisorb readily, although no studies have been reported. Thiols, being chemically similar to alcohols, are of interest as a potential means to achieve such functionalization. Second, adsorbed S is known to be effective in passivating surfaces of III–V materials, including GaN (e.g., ref 8). Adsorption of organosulfur compounds, together with thermal⁹ or photochemical¹⁰ dissociation, may provide a simple, vacuum-compatible method for delivering S to the GaN surface. Third, *n*-alkanethiols have been shown¹¹ to be useful in modifying metal/GaAs(100) barrier heights, which may be a viable approach to lowering the resistance of metal/*p*-GaN contacts. The structure of the film, such as the tilt angle of the thiol chain relative to the surface normal (which determines the effective thickness), is important in such applications.

We have approached this problem as one of quantitative surface analysis in ultrahigh vacuum (UHV) because wet-chemical techniques for producing atomically clean, stable,

and well-characterized GaN(0001) surfaces are not yet available. It is recognized that adsorption of *n*-alkanethiols from the vapor phase may not produce the well-ordered SAMs formed by adsorption from liquids.¹² Nevertheless, many of the applications envisioned for thiols on GaN involve adsorption under vacuum conditions. Furthermore, the *n*-alkanethiol/GaN system is especially interesting for this kind of study because the C KLL and N KLL features in X-ray-excited Auger electron spectroscopy (XAES) are well-separated yet occur in a kinetic energy (KE) region of fairly high surface sensitivity (200–400 eV). Hence, the relative intensities can be used for structure determination, once the adsorbate coverage has been obtained. Other substrates often used for SAMs (e.g., Au) do not exhibit similar conveniently placed XAES features of sufficient intensity.

Experimental Section

1. Reagents and Sample Preparation. 1-Octanethiol [1-OT, CH₃(CH₂)₆CH₂SH] was obtained commercially (Sigma-Aldrich, nominally 98.5% pure). The as-received reagent was checked by comparing the infrared spectrum (400–4000 cm^{–1}) of a 0.1-mm-thick liquid film (between KBr plates) with reference data.¹³ 1-OT was dried on an activated molecular sieve and degassed by repeated freeze–pump–thaw (FPT) cycles with freezing being done at dry-ice temperature. It was contained in a glass bulb (shielded from ambient light) on the dosing manifold, and a single FPT cycle was done at the start of each experiment to remove any H₂S that might arise from possible slow decomposition.¹⁴ The 1-OT room-temperature vapor pressure is ~430 mTorr, as was measured using the capacitance manometer on the dosing manifold. The GaN sample and the surface preparation method were the same as those used in an earlier study⁷ of H₂O adsorption. After cooling to <50 °C following annealing, the clean sample was exposed to 1-OT using a pinhole doser. During and after exposure the chamber viewports were covered and the nude ionization gauge was switched off to avoid possible excitation of the reagent vapor or the adsorbate.

2. Spectroscopic Techniques. All experiments were performed in a standard UHV chamber (base pressure ≈ 5 × 10^{–11} Torr). For XAES and X-ray photoemission spectroscopy (XPS), the excitation source (not monochromated) was either the Mg Kα_{1,2} line ($h\nu = 1253.6$ eV) or the Al Kα_{1,2} line ($h\nu = 1486.6$ eV). Because of the relevance to considerations of possible damage of the thiol layer during XPS (see the following), details of the Physical Electronics Model 04-548 source are given here. The

* Phone: +1-202-767-6728. E-mail: bermudez@estd.nrl.navy.mil.

- (1) Dubois, L. H.; Nuzzo, R. G. *Annu. Rev. Phys. Chem.* **1992**, *43*, 437.
- (2) Ulman, A. *Chem. Rev.* **1996**, *96*, 1533.
- (3) Poirier, G. E. *Chem. Rev.* **1997**, *97*, 1117.
- (4) Schreiber, F. *Prog. Surf. Sci.* **2000**, *65*, 151.
- (5) Swalen, J. D.; Allara, D. L.; Andrade, J. D.; Chandross, E. A.; Garoff, S.; Israelachvili, J.; McCarthy, T. J.; Murray, R.; Pease, R. F.; Rabolt, J. F.; Wynne, K. J.; Yu, H. *Langmuir* **1987**, *3*, 932.
- (6) Bermudez, V. M. *Surf. Sci.* **2002**, *499*, 109; (b) *Surf. Sci.* **2002**, *499*, 124; (c) *Surf. Sci.* **2002**, *519*, 173.
- (7) Bermudez, V. M.; Long, J. P. *Surf. Sci.* **2000**, *450*, 98.
- (8) Martinez, G. L.; Curriel, M. R.; Skromme, B. J.; Molnar, R. J. *J. Electron. Mater.* **2000**, *29*, 325.
- (9) Camillone, N., III; Khan, K. A.; Osgood, R. M., Jr. *Surf. Sci.* **2000**, *453*, 83.
- (10) Conrad, S.; Mullins, D. R.; Xin, Q.-S.; Zhu, X.-Y. *Appl. Surf. Sci.* **1996**, *107*, 145.
- (11) Nakagawa, O. S.; Ashok, S.; Sheen, C. W.; Martensson, J.; Allara, D. L. *Jpn. J. Appl. Phys.* **1991**, *30*, 3759.

(12) Schwartz, D. K. *Annu. Rev. Phys. Chem.* **2001**, *52*, 107.

(13) Integrated Spectral Data Base System for Organic Compounds (SDBS). <<http://www.aist.go.jp/RIODB/SDBS/menu-e.html>>.

(14) Shen, W.; Nyberg, G. L.; Liesegang, J. *Surf. Sci.* **1993**, *298*, 143.

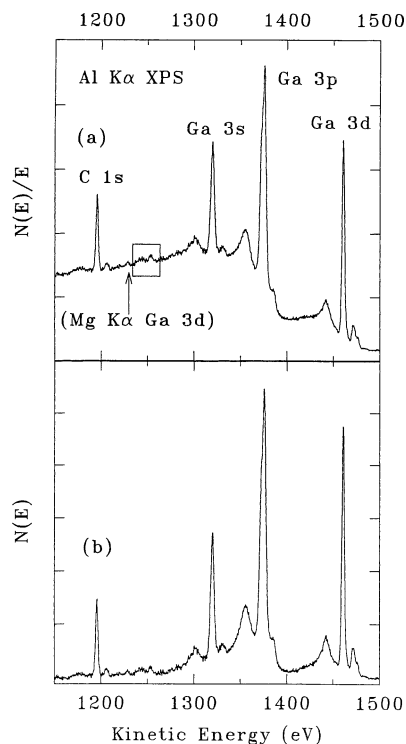


Figure 1. XPS spectra for a sample after a saturation dose of 1-OT. Part a shows the raw data, and part b shows the result of a Tougaard two-parameter background correction (see text) with $B = 2886$ and $C = 1634$ eV². The relative intensities in parts a and b are not quantitative, and both have been subjected to fifth-order, nine-point polynomial smoothing. The box encloses the S(2s) and Ga(L₁M₄₅M₄₅) features shown in more detail in Figure 2. The arrow indicates the Ga(3d) peak excited by K α emission from an Mg impurity in the Al anode.

anode, operated at 15 kV and 300 W, was equipped with a 2- μ m-thick Al foil window and positioned ~ 5 cm from the sample. The X-ray beam was incident at $\sim 60^\circ$ relative to the sample normal, and the absorbed flux was estimated¹⁵ to be about 2.1×10^{12} photons/(cm²·s). For ultraviolet photoemission spectroscopy (UPS), the source was a direct current discharge in He gas, and the absorbed flux¹⁵ was $\sim 3.3 \times 10^8$ photons/(cm²·s). Electron energy analysis was done with a double-pass cylindrical mirror analyzer (CMA) in the constant-resolution mode. The resolution was ~ 1.60 eV for XAES and ~ 1.75 eV for XPS (including the effect of finite X-ray line width). The UPS resolution was ~ 0.40 eV, determined largely by the CMA. Except where noted, methods involving electron excitation were avoided after thiol adsorption because of the susceptibility of these species to damage by the primary beam (ref 16 and works cited).

Results and Discussion

1. XPS and XAES Data. Figure 1a shows an XPS spectrum after a saturation dose (see below) of 1-OT. Adsorption occurs via the -SH group, as was expected, because equivalent doses of hydrocarbons such as ethane (C₂H₆), ethylene (C₂H₄), or benzene (C₆H₆) gave no C(1s) signal above the noise level (not shown). As in other XPS data^{17,18} for adsorbed 1-OT, the S(2s) and S(2p) peaks are weak relative to the C(1s). The S(2s) (Figure 2) lies just above the Ga(L₁M₄₅M₄₅) peak resulting from Auger decay of the photoionized Ga(2s) level [binding energy (BE) \approx

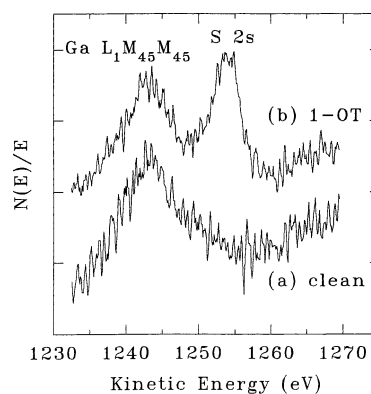


Figure 2. The region consisting of the Ga L₁M₄₅M₄₅ XAES and S(2s) XPS peaks, before and after dosing with 1-OT.

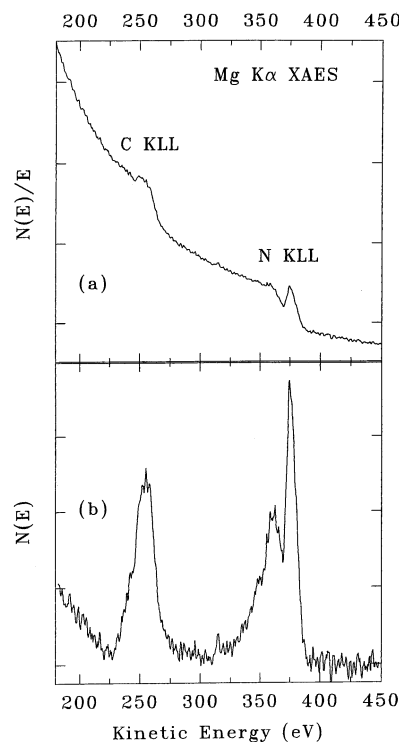


Figure 3. Similar to Figure 1 but showing the C KLL and N KLL XAES structure. Part a shows the raw data, and part b shows the result of a Tougaard three-parameter background correction with $B = 415$, $C = 551$, and $D = 436$ eV². The data have been subjected to fifth-order, nine-point polynomial smoothing. The feature near 320 eV is an artifact.

1299 eV]. It is noted that the Ga(L₁M₄₅M₄₅) energy of 1243 eV differs slightly from the empirical estimate¹⁹ of 1251 eV in elemental Ga. Based on the S 2s–2p BE difference of ~ 68 eV, the S(2p) lies on the high-KE edge of the Ga-(3s). Figure 3a shows the corresponding C KLL and N KLL XAES data. A detailed study of the adsorbate coverage versus the dose was not done, but the typical dose of $\sim 6 \times 10^{16}$ molecules/cm² was more than sufficient for quasi-saturation because the initial rapid uptake of 1-OT was complete at a much smaller dose. In terms of the langmuir unit (1 langmuir = 10^{-6} Torr·s), commonly used in exposure by backfilling, a 1-OT exposure of 1 langmuir would correspond²⁰ to a dose of 1.59×10^{14} molecules/cm².

(15) Long, J. P.; Bermudez, V. M. *Phys. Rev. B* **2002**, *66*, 121308.
 (16) Zharnikov, M.; Grunze, M. *J. Vac. Sci. Technol., B* **2002**, *20*, 1793.

(17) Hansen, H. S.; Tougaard, S.; Biebuyck, H. *J. Electron Spectrosc. Relat. Phenom.* **1992**, *58*, 141.

(18) Rieley, H.; Kendall, G. K.; Zemical, F. W.; Smith, T. L.; Yang, S. *Langmuir* **1998**, *14*, 5147.

(19) Coghlan, W. A.; Clausing, R. E. *A Catalog of Calculated Auger Transitions for the Elements*, ORNL-TM-3576; Oak Ridge National Laboratory: Oak Ridge, TN, 1971.

(20) Menzel, D.; Fuggle, J. C. *Surf. Sci.* **1978**, *74*, 321.

The C(1s) XPS spectrum showed no evidence of fine structure resulting from chemically distinct C atoms. Likewise, the Mg K α -excited Ga(2p) and N(1s) XPS (not shown) and the N KLL XAES data revealed no changes due to 1-OT. These null results parallel those for other organic adsorbates⁶ on this surface. The data were examined for loss of C due to damage by X-rays or by secondary electrons.^{16,21} Repeated scans of the C(1s) peak showed no significant loss of C in the time required (~30 min) to record a spectrum like that in Figure 1. However, after ~4 h of continuous X-ray irradiation (longer than the typical 2.5-hr period of data collection) a ~10–15% decrease in the C(1s) intensity was noted. A further discussion of possible damage effects follows. Slow desorption near room temperature was not a significant factor because raising the sample to ~120 °C caused only about a 10% loss of the C(1s) intensity (see below). It is noted that physisorbed *n*-alkanethiol layers on Au(111) exhibit a desorption peak near room temperature,²² which indicates that the species observed here are chemisorbed. Finally, XPS and electron-excited Auger electron spectroscopy (EAES) before dosing, and again after each series of experiments, showed the level of oxygen contamination to be at or below the detection limit of ~0.02 monolayers (MLs), where one ML is defined as one adsorbate per surface lattice site [1.135×10^{15} sites/cm² on GaN(0001)].

The adsorbate coverage and structure were quantified using the relative integrated intensities of the S(2s) and Ga(3s) XPS peaks and of the C KLL and N KLL XAES structures (see below). The approximate 1/KE dependence²³ of the CMA transmission on KE was taken into account in obtaining the area ratios. The pairs of spectra chosen for analysis are close in energy, which minimizes the error that would result from any residual KE dependence of the transmission. The S(2s) peak area was found by first subtracting the corresponding spectrum for the clean surface, scaled so as to minimize the Ga-(L₁M₄₅M₄₅) intensity in the difference. The S(2s) spectrum was then least-squares fitted with the sum of a Gaussian and a low-order polynomial background function, and the peak area was that of the fitted Gaussian.

The Ga(3s) is overlapped by the strong background of inelastically scattered Ga 3p and 3d photoelectrons. As is shown in Figure 1b, this background was greatly reduced using the procedure developed by Tougaard and Jansson.²⁴ The two-parameter universal scattering function²⁵ was used with the “*C*” term fixed at 1643 eV². The “*B*” term, which is a scaling factor needed to bring the background-corrected intensity to zero at energies well below the XPS structure, was found to be 2886 eV², very close to the optimum value²⁵ of 2866 eV². This indicates that the two-parameter function provides an adequate description of the background. After the background correction, the Ga(3s) peak area was obtained by least-squares fitting, as done previously, to separate it from the plasmon (~1300 eV) and Al K $\alpha_{3,4}$ (~1330 eV) satellites and from the background due to the Ga(3p) plasmon loss peak at ~1360 eV. With the resolution used here (see previous discussion) the weak S(2p) peak cannot be separated from the Ga(3s). Hence, the Ga(3s) area was corrected by assuming equal intensities^{17,18} for the S(2s) and S(2p) peaks.

Figure 3 shows the result of applying the background correction,²⁴ as was discussed previously, to the XAES

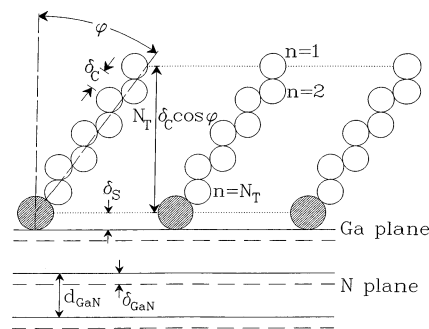


Figure 4. Schematic diagram showing the model for adsorbed 1-OT. Shaded and open circles show S and C, respectively, but hydrogens are not shown. S–C–C and C–C–C bond angles of 109° are used, and $n = 1$ corresponds to the outermost C atom. The alternating Ga- and N-layer structure of the wurtzite GaN lattice in the [0001] direction is indicated. Interplanar spacings and atomic diameters are approximately to scale.

data using the three-term scattering function²⁵ parametrized for organic polymers. Because of the relatively short effective electron attenuation lengths (EALs) for the C KLL and N KLL spectra (see appendix), much of the inelastic scattering occurs in the thiol layer. With the terms “*C*” and “*D*” fixed at 551 and 436 eV², respectively, the scaling factor “*B*” was found to be ~415 eV², close to the optimum polymer value²⁵ of 434 eV². This indicates that the three-term function provides an adequate description of the background, as was found²⁵ for *n*-alkanethiols on Au. The background remaining in the vicinity of C KLL and at a lower energy is due to the onset of slow-secondary electron emission and to the tail of the strong Ga(2p_{3/2}) peak at 132 eV, which are not included in the background correction. For N KLL, the area was determined by the numerical integration of the appropriate region of the background-corrected spectrum, Figure 3b.

The C KLL line shape, with an asymmetry at lower KE, is similar to that for gas-phase *n*-alkanes.²⁶ The area under the C KLL peak was obtained using two distinct methods. The first was by least-squares-fitting the background-corrected C KLL spectrum, Figure 3b, with a sum of two Gaussians and a low-order polynomial. The use of two Gaussians was simply an expedient means of fitting the C KLL shape to obtain the total area and has no other physical significance. In the second method, the raw spectrum of a clean surface [analogous to that in Figure 3a] was subtracted from that of the 1-OT-dosed surface, which removed the N KLL contribution together with most of the N KLL inelastic background and Ga(2p_{3/2}) and slow-secondary intensities at lower energy. The remaining spectrum (not shown) was dominated by the C KLL structure and its inelastic background. The background correction²⁴ was then applied, and the area was found by numerical integration. The final C KLL/N KLL area ratio for the two methods agreed to within ~10%, and the value used in the following is the average of the two.

2. Model for Adsorbed Thiol. Figure 4 shows a schematic model for the adsorbate, following Hansen et al.,¹⁷ which was used for the quantitative analysis of the data. The model will be summarized now, and details of the associated calculations will be given in the appendix. Here, δ_C is the increase in chain length per added C atom. Studies^{17,27,28} of the EAL versus the chain length in *n*-alkanethiol SAMs have used $\delta_C = 1.27$ Å. As in these

(21) Frydman, E.; Cohen, H.; Maoz, R.; Sagiv, J. *Langmuir* **1997**, *13*, 5089.

(22) Lavrich, D. J.; Wetterer, S. M.; Bernasek, S. L.; Scoles, G. J. *Phys. Chem. B* **1998**, *102*, 3456.

(23) Seah, M. P. *Surf. Interface Anal.* **1980**, *2*, 222.

(24) Tougaard, S.; Jansson, C. *Surf. Interface Anal.* **1993**, *20*, 1013.

(25) Tougaard, S. *Surf. Interface Anal.* **1997**, *25*, 137.

(26) Houston, J. E.; Rye, R. R. *J. Chem. Phys.* **1981**, *74*, 71.

(27) Laibinis, P. E.; Bain, C. D.; Whitesides, G. M. *J. Phys. Chem.* **1991**, *95*, 7017.

(28) Lamont, C. L. A.; Wilkes, J. *Langmuir* **1999**, *15*, 2037.

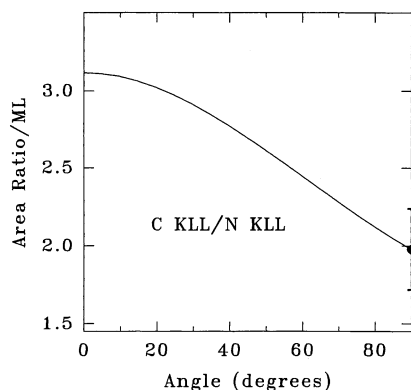


Figure 5. Mg K α -excited C KLL/N KLL XAES area ratio versus the tilt angle (cf. Figure 4), computed for one ML of densely packed 1-OT adsorbed on GaN(0001). The point shows the experimental value, scaled for the measured 1-OT coverage. The error bar is obtained from the statistical variance derived from repeated measurements and added in quadrature to the uncertainty due to that in the coverage determination. See the text and appendix for details.

studies, the attenuation of underlayer XPS and XAES intensities was computed by treating the alkyl layer as a continuum of closely packed C atoms with an effective thickness of $N_T \delta_C \cos \phi$ (where N_T is the number of C atoms in the chain). The C KLL XAES intensity was computed by summing the contribution from each C in the chain, weighted by the attenuation due to upper C atoms. A similar approach has been used^{17,28} to model the dependence of the C(1s) XPS intensity on the chain length for *n*-alkanethiol SAMs on Au. The term δ_S is the effective height of the S atom above the surface Ga plane and, in the model, also represents the minimum effective layer thickness for alkyl chains lying flat on the surface ($\phi = 90^\circ$). In EAL studies,^{27,28} δ_S corresponds to the small attenuation effect that is independent of the chain length. Here, $\delta_S \approx 1 \text{ \AA}$ is used, which is approximately the atomic radius of the S atom. It will be seen below that the exact value of δ_S has little effect on the final results of the analysis.

Figure 4 indicates that the maximum attainable thiol coverage increases as ϕ decreases and more surface sites become accessible. However, as will be shown in the following, the thiol coverage can be estimated independently of ϕ . With this model and the procedure described in the appendix, peak area ratios were computed versus ϕ and versus the thiol saturation coverage, Θ_T^S . The model gives no information concerning the twist angle¹ of the chain about the axis nor any details of the chemical interaction between S and Ga.

The saturation thiol coverage can be obtained independently of ϕ from the S(2s)/Ga(3s) area ratio (0.053 ± 0.005 , average of four runs) because both peaks are attenuated nearly equally by the hydrocarbon layer, whatever its structure. The result, $\Theta_T^S = 0.28 \pm 0.03 \text{ ML}$, is at the low end of the range (0.29 to 0.40 ML) found for a wide variety of adsorbates^{6,7} on this surface. The C KLL/N KLL area ratio (0.524 ± 0.06 , average of seven runs) depends on both Θ_T^S and ϕ . This ratio was computed for $\Theta_T^S = 1 \text{ ML}$ (as was defined previously) versus ϕ with the results shown in Figure 5. The measured area ratio was then scaled by the saturation coverage, $\Theta_T^S = 0.28 \text{ ML}$, to obtain the data point shown. Taking into account the error bar, the result indicates a tilt angle of $\geq 72^\circ$ with a most probable value of 90° .

In principle, the C(1s)/Ga(3s) XPS area ratio could also be used, but the surface sensitivity is poor because the

C(1s) and Ga(3s) EALs (see appendix) are significantly greater than the chain length. This makes the dependence of the C(1s)/Ga(3s) ratio on the tilt angle much weaker than that of the C KLL/N KLL ratio. As a check, the C/S atom ratio (i.e., N_T) was estimated using $N_T = [I_{C(1s)}/I_{S(2s)}] - [\sigma_{S(2s)}/\sigma_{C(1s)}]$, which applies to a flat-lying monothiol chain. Here, I_x and σ_x are, respectively, XPS integrated intensities and photoionization cross sections (see appendix). A discrepancy was found, giving $N_T \approx 10.9 \pm 0.7$ versus the true value of 8. A similar effect has occurred in studies of *n*-alkanethiols on Au, using $I_{C(1s)}/I_{S(2p)}$. Himmel et al.²⁹ found an N_T of 8 ± 1 for a C₇ chain, and Ishida et al.³⁰ found ~ 7.4 for a C₄ chain. A likely cause, at least in the present work, is an error in determining $I_{S(2s)}$, which is very small (cf. Figure 1). If the discrepancy were removed by arbitrarily increasing $I_{S(2s)}$ and, thereby, the estimated Θ_T^S (to $\sim 0.39 \text{ ML}$), the effect on Figure 5 would be to decrease the data point to ~ 1.5 . This would not change the basic conclusion that $\phi \approx 90^\circ$ best accounts for the data.

Geometry indicates that the "footprint" of a flat-lying and straight 1-OT molecule (all-trans, as in Figure 4) is approximately 54.7 \AA^2 . This is the product of a length³¹ of 12.9 \AA and a width of 4.24 \AA (representing the minimum intermolecular spacing)¹ and corresponds to a maximum coverage of 1.83×10^{14} molecules/cm², or $\Theta_T^S = 0.16 \text{ ML}$. Furthermore, with a Ga–Ga nearest-neighbor distance of 3.189 \AA , each such thiol would block the adsorption site and four others, giving 0.20 ML for a maximum coverage (independently of the restriction imposed by the molecular packing density). Both these values appear to be inconsistent with the present estimate of $\Theta_T^S = 0.28 \pm 0.03 \text{ ML}$.

The present results for the coverage and tilt angle can be reconciled with the molecular "footprint" given above if 1-OT assumes a configuration resembling the δ phase reported^{32,33} by Poirier et al. for decanethiol on Au(111). This involves a deviation from strict two-dimensionality (termed "out-of-plane interdigitation") in which some alkyl chains lie partially on top of others, with all S atoms still bonded to the surface. An alternative model, based on a bilayer with a physisorbed second layer, is unlikely because of the previously noted low (i.e., below $\sim 50^\circ \text{ C}$) desorption maximum for such weakly bonded *n*-alkanethiol layers.

The tilt angle obtained here, $\phi \approx 90^\circ$, is larger than the result³⁴ for a CH₃(CH₂)₁₆CH₂SH SAM on GaAs(100) ($\phi = 57 \pm 3^\circ$) and much larger than the value¹ of $\phi \approx 30^\circ$ for *n*-alkanethiol SAMs on Au. However, *n*-alkanethiols with six-, seven- or nine-carbon chains have been found^{29,32,33,35} to adsorb in a lying-down geometry on Au(111) at a low coverage and in a tilted upright configuration at saturation. In all cases, the lying-down *n*-alkanethiol chains were found to be straight, as are modeled in Figure 4.

3. Annealing Effects. The effect of annealing the saturated layer was investigated using the C KLL/N KLL area ratio, and the results are summarized in Figure 6. The sample was raised to each temperature, the heater

(29) Himmel, H.-J.; Wöll, Ch.; Gerlach, R.; Polanski, G.; Rubahn, H.-G. *Langmuir* **1997**, *13*, 602.

(30) Ishida, T.; Nishida, N.; Tsuneda, S.; Hara, M.; Sasabe, H.; Knoll, W. *Jpn. J. Appl. Phys.* **1996**, *35*, L1710.

(31) Bain, C. D.; Troughton, E. B.; Tao, Y.-T.; Evall, J.; Whitesides, G. M.; Nuzzo, R. G. *J. Am. Chem. Soc.* **1989**, *111*, 321.

(32) Poirier, G. E. *Langmuir* **1999**, *15*, 1167, 3018.

(33) Poirier, G. E.; Fitts, W. P.; White, J. M. *Langmuir* **2001**, *17*, 1176.

(34) Sheen, C. W.; Shi, J.-X.; Mårtensson, J.; Praikh, A. N.; Allara, D. L. *J. Am. Chem. Soc.* **1992**, *114*, 1514.

(35) Kondoh, H.; Kodama, C.; Sumida, H.; Nozoye, H. *J. Chem. Phys.* **1999**, *111*, 1175.

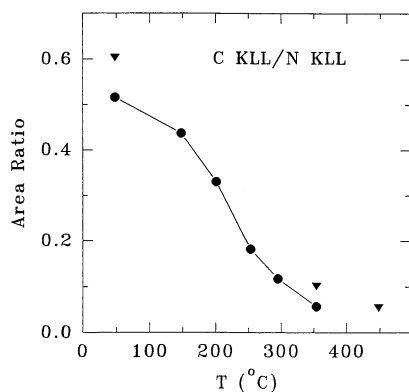


Figure 6. C KLL/N KLL XAES area ratio versus annealing. The ratio is the observed value, not scaled for coverage as in Figure 5. The solid line connecting the points is simply a visual aid, and different symbols show data from different runs.

was switched off, and XAES data were collected during cooling. Figure 5 shows that an increase in the C KLL/N KLL ratio would indicate the reorientation of the thiol chain away from a flat configuration, a possible first step in the formation of a SAM. On the other hand, a decrease could be caused only by desorption or decomposition. The results show a monotonic loss of C with a maximum desorption rate in the 200–250 °C range, although the relative importance of the C–C versus S–C bond dissociation in the loss of C cannot be determined at present. A qualitatively similar loss in intensity was observed in comparing the C(1s) XPS data (not shown) before annealing and after the last anneal. Following the last anneal, the S(2s)/Ga(3s) area ratio (spectra not shown) indicates an ~20% loss of S relative to an unannealed sample (vs a factor of ~10 reduction in C coverage shown in Figure 6). This indicates that a significant fraction of the S remains bonded to the surface under these conditions. Finally, the comparison shown in Figure 6 between the effects of annealing in one, versus several, steps suggests that the intensity change is due to temperature rather than to the cumulative effect of X-ray radiation damage in successive scans.

The loss of some S, as well as the continued slow loss of C up to 450 °C (the highest temperature studied), suggests the occurrence of competing reactions in addition to the main thermal effect. Such processes could include, for example, desorption of intact 1-OT molecules (as a means of losing S as well as C) or adsorption of thermally generated hydrocarbon fragments on the GaN surface (as a means of C retention at a high temperature). Previous work⁹ on the interaction of CH₃SH with the GaAs(110) surface shows predominantly desorption of the intact molecule, from a chemisorbed state, at slightly above room temperature. Bonding in the case of GaAs(110) is believed to involve the donation of S nonbonding electrons to the empty Ga dangling orbital.⁹ The apparently different behavior for 1-OT on the Ga-polar GaN(0001) surface could be due to a number of effects that cannot be defined at present. These include reactive surface defects (i.e., N vacancies) or the higher ionicity of the Ga–N versus Ga–As bond.

4. UPS Data. The issue of possible damage to the thiol layer during XPS data collection will now be examined using the He(II) UPS data shown in Figure 7. The spectrum for the clean surface has been discussed elsewhere (e.g., ref 7 and works cited). The strong peak at ~15 eV is the “Ga(3d) level” [properly described³⁶ as the nonbonding Ga(3d) state], and the weak, broad feature near 18 eV is the “N(2s) level” [properly described³⁶ as the

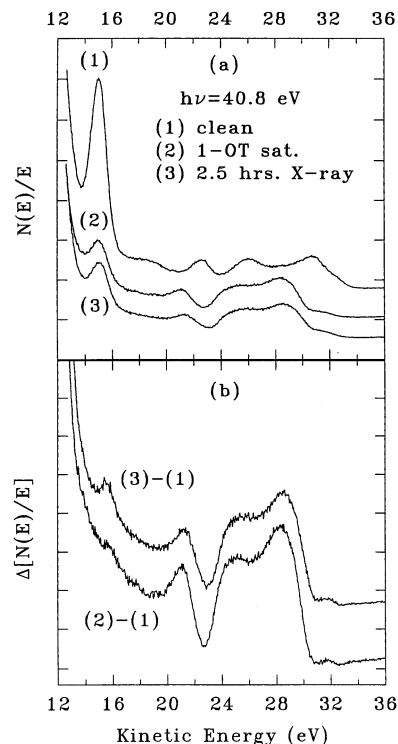


Figure 7. He(II) UPS data showing (a) the effect of 1-OT adsorption on the clean surface and subsequent X-ray irradiation and (b) the corresponding difference spectra. Trace 1 is for the clean surface, trace 2 is the spectrum after a saturation dose of 1-OT, and trace 3 shows the effect of a subsequent 2.5-hr exposure to X-ray radiation. Each trace is the average of two scans (not smoothed) and has been displaced vertically for clarity.

Ga(3d)–N(2s) antibonding state]. The peak near 22.5 eV is a “ghost” of the Ga(3d) excited by the $h\nu = 48.4$ eV satellite of the main He(II) line at $h\nu = 40.8$ eV. The rapidly rising intensity toward low KE is due to secondary electrons and to emission excited by the much stronger He(I) line ($h\nu = 21.2$ eV).

Upon 1-OT adsorption, the substrate emission is strongly attenuated, as is shown by the loss in Ga(3d) intensity, and the resulting spectrum is then dominated by adsorbate features. In principle, the Ga(3d) attenuation could be used as a check of the adsorbate layer thickness. However, the lack of a reliable *n*-alkanethiol EAL for electron kinetic energies above 1.5 eV (ref 37) and below 50 eV (ref 28) prohibits this. Prolonged X-ray exposure under the conditions used for XPS leads to, perhaps, a slight increase in the Ga(3d) intensity, which suggests a possible slight loss of adsorbate material.^{16,21} This would be consistent with the corresponding small decrease in the C(1s) XPS intensity noted previously.

It has also been shown²¹ that damage can take the form of structural changes not necessarily detectable as a loss of C atoms. To address this issue, difference data were obtained by subtracting the clean-surface spectrum, scaled so as to minimize the Ga(3d) intensity in the difference. The feature near 15 eV is close to the Ga(3d), and the structure in this part of the spectrum is difficult to obtain reliably in the differences. The weak background emission above ~32 eV arises from excitation by the 48.4 eV He(II) satellite, as was described previously.

(36) Dudešek, P.; Benco, L.; Daul, C.; Schwarz, K. *J. Phys.: Condens. Matter* **1998**, *10*, 7155.

(37) Monjushiro, H.; Watanabe, I. *Anal. Sci.* **1995**, *11*, 797.

The major structure, in the 20–30 eV range, is due to the 1-OT valence orbitals and shows little or no X-ray-induced change other than a slight broadening. In particular, formation of C=C bonds due to the loss of H would result in the growth of a band due to the π orbital. This is the highest occupied molecular orbital (HOMO) of a simple alkene and lies well above the bands due to σ -bonding orbitals.³⁸ For free *n*-alkanethiols,^{38,39} the S nonbonding orbital is the HOMO and also produces a narrow and intense band lying above the σ -bonding orbitals. Such a feature appears to be absent for 1-OT adsorbed on GaN(0001), consistent with bonding via the thiol group. However, the exact nature of the adsorbate–surface bond is unclear at present.

It, thus, appears that 1-OT layers on GaN(0001) are less susceptible to damage during XPS than are typical *n*-alkanethiols on Au. This result is similar to that found⁴⁰ in a comparison of Au and InP substrates, for which it was suggested that a difference in the yield or energy distribution of secondary electrons may be important.

Summary and Conclusions

The present work, together with previous results⁶ for amine chemisorption, provides an array of surface chemistries suitable for functionalizing the Ga-polar GaN(0001) surface. In addition to amines and thiols, it seems likely that organic alcohols could also be used for this purpose, given the chemical similarity between alcohols and thiols and the high reactivity⁷ of H₂O with this surface. With the use of quantitative analysis of the XPS and XAES intensities, it was found that 1-OT adsorbs from the vapor phase via the thiol group with a saturation coverage of ~ 0.28 MLs and with the alkyl chain lying essentially parallel to the surface. Annealing a saturated surface above ~ 250 °C leads to the loss of a large fraction of initial C but a much smaller fraction of S. It was also found using UPS that, for 1-OT on GaN(0001), little or no damage occurs during XPS under the conditions used here. Finally, it was shown that C KLL XAES results can, in favorable situations, be a useful supplement to more widely reported C(1s) XPS data.

It remains to be determined whether SAM formation on this surface can be induced by adsorption of thiols from liquid media or by very large doses in UHV. The detailed nature of the S–Ga chemical bond at the surface is also unknown at present.

Acknowledgment. This work was supported by the Office of Naval Research. A. D. Berry is thanked for drying the thiol, and J. W. P. Hsu is thanked for suggesting this problem. The GaN sample was kindly provided by D. D. Koleske and A. E. Wickenden. D. Y. Petrovykh is thanked for enlightening discussions on thiol adsorption and for a critical reading of the manuscript. Thanks are also due to a referee for pointing out an error in the original estimate for the 1-OT “footprint” and for calling attention to ref 32.

Appendix

This section describes the procedure for the quantitative analysis of the XPS and XAES peak area ratios. With reference to Figure 4, the Ga(3s) and S(2s) XPS and the C KLL and N KLL peak areas are given by

$$I_{\text{Ga}(3s)} = \sigma_{\text{Ga}(3s)} \left[\sum_{n=0}^{\infty} \exp(-nd_{\text{GaN}}/\lambda_{\text{GaN}} \cos \alpha) \right] \times \exp[-(\delta_{\text{S}} + N_{\text{T}}\delta_{\text{C}} \cos \phi)/\lambda_{\text{T}} \cos \alpha] \quad (1)$$

$$I_{\text{S}(2s)} = \Theta_{\text{T}}^{\text{S}} \sigma_{\text{S}(2s)} \exp(-N_{\text{T}}\delta_{\text{C}} \cos \phi/\lambda_{\text{T}} \cos \alpha) \quad (2)$$

$$I_{\text{CKLL}} = \Theta_{\text{T}}^{\text{S}} \sigma_{\text{C}(1s)} \rho_{\text{CKLL}} \times \sum_{n=1}^{N_{\text{T}}} \exp[-(n-1)\delta_{\text{C}} \cos \phi/\lambda_{\text{T}} \cos \alpha] \quad (3)$$

$$I_{\text{NKLL}} = \sigma_{\text{N}(1s)} \rho_{\text{NKLL}} \exp(-\delta_{\text{GaN}}/\lambda_{\text{GaN}} \cos \alpha) \times \left[\sum_{n=0}^{\infty} \exp(-nd_{\text{GaN}}/\lambda_{\text{GaN}} \cos \alpha) \right] \exp[-(\delta_{\text{S}} + N_{\text{T}}\delta_{\text{C}} \cos \phi)/\lambda_{\text{T}} \cos \alpha] \quad (4)$$

The σ_{k} 's are photoionization cross sections at the appropriate X-ray energies, given independently by Scofield (ref 41) and Band et al. (ref 42). The relative σ_{k} 's of interest are practically identical in both tabulations, and recent work⁴³ verifies the accuracy of the values used here. The saturation thiol coverage, $\Theta_{\text{T}}^{\text{S}}$, was defined previously, and $\alpha = 42^\circ$ is the CMA collection angle. The ρ_{KLL} terms are the total Auger decay probabilities (neglecting fluorescence decay) of the C(1s) and N(1s) core holes. These are nearly equal, and the empirical values⁴⁴ of Ebel et al. were used here. The interplanar spacings, $d_{\text{GaN}} = 2.59$ Å and $\delta_{\text{GaN}} = 0.648$ Å, are defined in Figure 4 and obtained from crystallographic data. The effective EAL in the thiol layer (or in GaN) is given by λ_{T} (or λ_{GaN}). The terms δ_{S} and δ_{C} , defined in Figure 4, were given previously.

Only relative intensities are used here, and the CMA in constant-resolution mode detects electrons of fixed energy. Hence, factors relating to X-ray flux and detector efficiency are suppressed, and the raw data have already been corrected for the $1/\text{KE}$ dependence of the CMA transmission. The XPS asymmetry factor,²³ which has also been omitted, is the same for all s levels measured under the same conditions and cancels in the ratio. The atomic subshell occupancy ($n = 2$ for all s levels) has also been omitted. In the KLL intensities, the effect of bremsstrahlung in producing core holes⁴⁵ is neglected because it is small and nearly the same for Mg K α excitation of C(1s) and N(1s). Finally, the Ga and N planes contain equal numbers of atoms; hence, these quantities are also omitted.

In eqs 1 and 4, the Σ term gives the sum of contributions from each Ga or N plane, and terms in λ_{T} give the attenuation by the thiol adlayer. In eq 2, the exponential gives the attenuation by the $N_{\text{T}} = 8$ carbon layers, and in eq 3, the Σ term gives the contribution from these layers. The term in δ_{GaN} in eq 4 gives the (small) attenuation by the terminating Ga layer.

Semiempirical λ_{T} and λ_{GaN} values (Table 1) were obtained from the National Institute of Standards and

(41) Scofield, J. H. *J. Electron Spectrosc. Relat. Phenom.* **1976**, *8*, 129.

(42) Band, I. M.; Kharitonov, Yu. I.; Trzhaskovskaya, M. B. *At. Data Nucl. Data Tables* **1979**, *23*, 443.

(43) Seah, M. P.; Gilmore, I. S.; Spencer, S. J. *J. Electron Spectrosc. Relat. Phenom.* **2001**, *120*, 93.

(44) Ebel, H.; Ebel, M. F.; Krocza, H. *Surf. Interface Anal.* **1988**, *12*, 137.

(45) Ebel, H.; Ebel, M. F.; Wernisch, J.; Wiederschinger, H. *J. Electron Spectrosc. Relat. Phenom.* **1993**, *62*, 359. Ebel, M. F.; Ebel, H.; Wernisch, J.; Kricza, H.; Etmayer, P. *Surf. Interface Anal.* **1988**, *12*, 175.

(38) Kimura, K.; Katsumata, S.; Achiba, Y.; Yamazaki, T.; Iwata, S. *Handbook of HeI Photoelectron Spectra of Fundamental Organic Molecules*; Japan Scientific Societies Press: Tokyo, 1981.

(39) Ogata, H.; Onizuka, H.; Nihei, Y.; Kamada, H. *Bull. Chem. Soc. Jpn.* **1973**, *46*, 3036.

(40) Zerulla, D.; Chassé, T. *Langmuir* **1999**, *15*, 5285.

Table 1. Effective EALs Used in the Data Analysis^a

quantity	KE (eV)	EAL (Å)
λ_T (eq 3)	255 (C KLL)	11.0
λ_T (eq 4)	375 (N KLL)	14.6
λ_T (eq 2)	1254 [S (2s)]	39.8
λ_T (eq 1)	1320 [Ga(3s)]	41.7
λ_{GaN} (eq 4)	375 (N KLL)	7.27
λ_{GaN} (eq 1)	1320 [Ga (3s)]	22.0

^a λ_T and λ_{GaN} refer to the attenuation length in the *n*-alkanethiol layer and in GaN, respectively.

Technology database.⁴⁶ The λ_T values were computed using parameters⁴⁷ for *n*-paraffin (C₂₆H₅₄), a solid hydrocarbon. As a test, values thus obtained at 1150 and 1400 eV (35.5 and 41.8 Å, respectively) were close to experimental results based on the attenuation of the Al K α -excited 4d and 4f XPS peaks of a Au substrate by *n*-alkanethiol SAM layers [37 and 45 Å (ref 17); 34 \pm 1 and 42 \pm 1 Å (ref 27)]. As a further test, similar comparisons were done at a lower KE. At 200 and 350 eV, λ_T values of 9.08 and 13.6 Å, respectively, were computed versus the experimental results²⁸ of 9.1 \pm 1 and 12.4 \pm 1 Å. To our knowledge, there is only one report⁴⁸ of EALs in GaN. The calculated λ_{GaN} at 970 eV was 15.4 Å versus the experimental result of 20 \pm 1 Å.

(46) Powell, C. J.; Jablonski, A. *NIST Electron Effective-Attenuation-Length Database, Vers. 1.0*; National Institute of Standards and Technology: Gaithersburg, MD, 2001; *Surf. Interface Anal.* **2002**, *33*, 211. See <http://www.nist.gov/srd/nist82.htm> for information on obtaining this database.

(47) Tanuma, S.; Powell, C. J.; Penn, D. R. *Surf. Interface Anal.* **1993**, *21*, 165.

(48) Lu, J.; Haworth, L.; Westwood, D. I.; Macdonald, J. E. *Appl. Phys. Lett.* **2001**, *78*, 1080. Note that the authors term their result an "inelastic mean-free path" (IMFP). However, the method of measurement conforms to that of an EAL. The distinction between IMFP and EAL is discussed in ref 46.

With elastic scattering included,⁴⁶ λ in XPS depends on the angles made by the surface normal with the incident X-rays and with the photoelectron path. The λ_T calculations noted above were performed for the same geometric conditions as the experiments and include the asymmetry parameters⁴⁹ for the Au(4d) and Au(4f) peaks as appropriate. In the present work, the X-rays were incident at $\sim 60^\circ$ relative to the sample normal, and the XPS λ values in Table 1 are averages over the CMA collection aperture. The variation over the CMA aperture is about $\pm 5\%$ for the XPS λ_T values and about $\pm 10\%$ for the Ga(3s) λ_{GaN} .

As was noted in the text, a value of $\delta_S = 1$ Å was used, and a more accurate value cannot be obtained without a detailed model for the geometry of the adsorption site. An upper limit on δ_S would be ~ 2.3 Å, the sum of the covalent radii of Ga and S. Varying δ_S over a range of 0 to 2.3 Å caused a change of only about $\pm 10\%$ in the computed C KLL/N KLL ratio, which is within the experimental error of the data point (Figure 5), and had essentially no effect on the computed S(2s)/Ga(3s) ratio from which Θ_T^S was obtained.

With all the terms in eqs 1–4 now defined, Θ_T^S can be obtained from $I_{\text{S}(2s)}/I_{\text{Ga}(3s)}$ and the plot in Figure 5 generated. The data reduction procedure was tested previously⁵⁰ using the N KLL/Ga LMM area ratio in EAES for an atomically clean GaN(0001) surface in an UHV. The N/Ga atom ratio thus obtained for bulk GaN was within a few percent of unity.

LA030032A

(49) Reilman, R. F.; Msezane, A.; Manson, S. T. *J. Electron Spectrosc. Relat. Phenom.* **1976**, *8*, 389.

(50) Bermudez, V. M. *J. Appl. Phys.* **1996**, *80*, 1190.